April 2006

Modeling the effect of the separation of gas stream from droplet stream on the growth rate of transformed roots of Artemisia annua in a nutrient mist bioreactor

Lindsay A. Bulso
Worcester Polytechnic Institute

Project Number: PZW4984

Modeling the effect of the separation of gas stream from droplet stream on the growth rate of transformed roots of *Artemisia annua* in a nutrient mist bioreactor.

A Major Qualifying Project Report:

submitted to the Faculty

of the

WORCESTER POLYTECHNIC INSTITUTE

in partial fulfillment of the requirements for the

Degree of Bachelor of Science

by

_____

Lindsay A. Bulso

Date: Apr 27, 2006

Approved:

_____

Professor Pamela J. Weathers, Primary but Co-Advisor

_____

Professor Terri Anne Camesano, Major Advisor

Acknowledgements

Barbara Wyslouzil for explaining to the mist deposition model to me and also for aiding in the design of the reactor.

Melissa Towler for sterilization of the misting system and general lab assistance.

Martin Driggs for teaching me how to make media, culture roots, and use proper sterile technique.

Giacomo Ferraro for assisting in the construction of the reactor and also for letting me borrow some of his tools.

Table of Contents

List of Illustrations

List of Tables

1. ABSTRACT

Previous nutrient mist bioreactors used ultrasonic misting to generate fine droplets, but are not scaleable. Thus, to scale-up root cultures, a new misting system must be used. The new system uses a spray nozzle that produces very fine droplets that are not slaved to the air stream for deposition. Air, however, is crucial for root growth. This project used our mist deposition model to predict how the separation of the air from the mist droplets might alter root growth.

2. INTRODUCTION

2.1 There is an increased demand for artemisinin

Every year, millions of people die from malaria, a disease that is caused by the parasite *Plasmodium falciparum* [Ferreira, et al., 2005]. These parasites are carried by mosquitoes, which bite and infect humans. Although mosquito nets are in place to minimize bites, the annual number of deaths is still large, which shows that it is important to have a cure for this disease. Quinine and quinine-derived medicines have been used to treat malaria for hundreds of years, but these treatments have become more and more ineffective as resistant parasites have developed [Ferreira, et al., 2005]. As the need for new treatments arose, the World Health Organization (WHO) recommended artemisinin-combination treatments (ACT) as a new option for treating malaria [Ferreira, et al., 2005].

The current supply of artemisinin is not sufficient to meet the demand. The WHO predicted that 130-220 million ACT would be needed in 2005, while estimates only show enough artemisinin for 30 million ACT available [Ferreira, et al., 2005]. Artemisinin is a secondary metabolite produced by the Qinghao plant, *Artemisia annua* [Ferreira, et al., 2005]. This plant produces the compound in small quantities. Secondary metabolites are often quite difficult to produce via organic synthesis due to complicated structures and chirality [Kim, et al., 2002b], but many of them, including artemisinin are very useful. Important plant-made chemicals include taxol and tricosanthin which are anti-cancer and anti-AIDs drugs, respectively [McKelvey, et al., 1993]. Because these secondary metabolites are so useful and difficult to produce, ways of increasing secondary metabolite production *in planta* and ways to mass-produce the plants that make these metabolites are important [McKelvey, et al., 1993]. Transformed root cultures offer a rapidly growing plant production system [Wyslouzil., et al., 1997; Carvalho and Curtis, 1998; Kim, et al., 2001]. This project focuses on modeling the growth of transformed (hairy) roots of *Artemisia annua* in a new version of a nutrient mist bioreactor.

2.2 It is advantageous to grow roots in a gas-phase reactor rather than a liquid-phase reactor.

Although it has been shown that roots grow well in shake flasks, growth is limited due to oxygen deprivation [Weathers, et al., 1999], which limits aerobic respiration [Kim,

et al., 2002a]. Poor oxygen distribution is common to liquid-phase reactors due to the low solubility of oxygen in the medium [Carvalho, et al., 1998]. The effects of oxygen deprivation are magnified when the reactor volume increases, and also when the density of the root bed increases [Kim, et al., 2002a]. Therefore, in liquid-phase reactors, as time progresses, and the bed density increases, the growth rate will decrease due to an insufficient oxygen supply in the core of the bed.

Roots grown in gas-phase reactors are constantly exposed to the gas-phase nutrients, and liquid medium is provided as a mist [Kim, et al., 2002b]. In gas-phase reactors, growth rates should therefore, remain constant [Kim, et al., 2002a]. McKelvey, et al. (1993) investigated root growth in various liquid- and gas-phase reactors by comparing biomass accumulation in submerged air-sparged reactors (where gas-phase nutrients were poorly distributed), trickle-bed reactors, and inclined reactors. The inclined reactor was set up similarly to the trickle-bed, but was slanted at a 15 degree angle above horizontal to create an uneven distribution of nutrients, which forced the roots to transport liquid nutrients to those that were not in contact with the liquid. Roots grew better in the inclined reactor than the air-sparged reactor, which demonstrated that roots can compensate for poor liquid distribution better than they can for poor gas distribution. These results show the potential for gas-phase bioreactors.

Because of the ample oxygen supply in gas-phase reactors, roots perform aerobic respiration, which produces more energy than anaerobic respiration [Towler, 2006]. Therefore, roots grown in gas-phase reactors should also be able to produce more secondary metabolites [Towler, 2006]. Indeed, it has been shown that roots grown in gas-phase reactors do produce more artemisinin than roots grown in liquid-phase reactors [Kim, et al., 2002a]. Others have also shown that roots produce more secondary metabolites in highly aerated reactors. For example, Flores and Curtis (1992) showed that *H. muticus* roots produced 3.5 times more solavetivone in trickle-bed reactors than in submerged reactors.

Work has been done to try to eliminate the oxygen supply problem in liquid-phase reactors. One kind of reactor studied is the bubble column, in which roots are dispersed in media and oxygen is bubbled up through the bed. At high bed densities, however, this

does not provide adequate bulk mixing [McKelvey, et al., 1993; Kim, et al., 2002b]. Channeling often occurs, resulting in localized oxygen deprivation [Kim, et al., 2002b].

Another type of liquid-phase reactor studied is the convective flow reactor. In this type of reactor, culture medium is oxygenated in a stirred-tank, and then pumped up through the bed [Carvallo and Curtis, 1998]. Convective flow reactors were shown to be successful for growing roots, but are not practical for scale-up due to large pressure required to force liquid up through the bed. [Flores and Curtis, 1992; Singh and Curtis, 1994; Carvallo and Curtis, 1998].

2.3 A nutrient mist reactor will be more effective than a trickle-bed reactor.

Studies have also been done using trickle-bed reactors, which are similar to nutrient mist bioreactors. The major difference is that the average droplet size is much larger. Mists are generally characterized by droplets of 0.01-10μm, while sprays have droplets of 10-10,000μm (Figure 2.3.1) [Weathers and Wyslouzil, 2000]. Segregation of mists, fogs, and sprays by droplet size is rather vaguely defined and overlap exists between these categories especially in the range of 5-40 μm (Perry and Green, 1997). Large droplet sizes can lead to decreased reactor performance because the droplets are more easily trapped by the root bed. As the droplets are captured and coalesce, the reactor becomes a liquid-phase reactor, and oxygen mass transfer starts to become limited. This results in decreased root growth.

Williams and Doran (2000) tested the performance of trickle bed reactors with droplets of about 125μm, and found that reactor performance decreased when liquid distribution was not uniform over and through the bed. Most of the liquid coalesced and traveled through the bed as trickling rivulets (Williams and Doran, 2000). This resulted in channeling and an uneven distribution of nutrients. Ramakrishnan and Curtis (2004) worked with a 14-L trickle-bed reactor and droplets of about 525μm, and found significant liquid hold up. In nutrient mist reactors, the mist droplets are much smaller (0.5-30μm), and they are carried by the air through the bed as opposed to being dropped onto the bed. This leads to a more even distribution of media throughout the root bed, and there is less liquid hold-up.

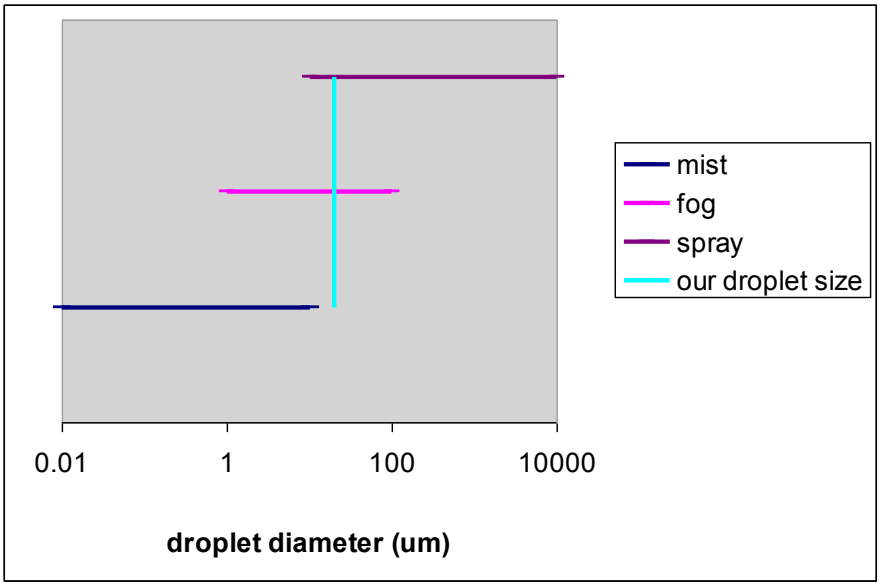

Figure 2.3.1. Droplet sizes for mist, fog, and spray.

Williams and Doran (2000) also showed that trickle-bed reactors are inefficient at high bed densities. The droplets are too large to get through the bed and to the roots in the dense core. After about 10 days of running their reactor, the roots in the core became callused. After about 25 days, the roots were completely black, which showed that adequate nutrients were not reaching the core, and that smaller droplets were needed to penetrate dense beds. Taken together these studies show that trickle-beds revert to liquid-phase reactors once the density of the root bed gets too high [Williams and Doran, 2000]. This is likely the results of the large droplet size used in these studies.

2.4 The aerosol model

In contrast to a liquid phase reactor, oxygen is not limiting in a gas phase reactor. However, the availability of liquid nutrients may limit growth if mist droplets do not reach the surface of all roots, or if an inadequate number of droplets are fed to the root bed. Therefore, understanding how mist droplets are deposited in the reactor is important for optimizing reactor performance. A model, based on droplet capture through fibrous filters, has been developed by Wyslouzil, et al. (1997) to explain mist deposition. To develop this model, a reactor was used in which mist droplets were generated by an ultrasonic transducer and then carried to the root bed by air flow.

In this model, it was assumed that hairy root beds would act similarly to fibrous filters with respect to mist deposition. So, methods for describing mist deposition in

fibrous filters were used as a starting point. The main differences between roots and fibers in a filter are their structure and their arrangement. Hairy roots have lateral roots that branch off of the primary root and even other lateral roots. Hairy roots also have root hairs that project radially from the primary root. Filter fibers have neither of these features. Also, filter fibers are purposely arranged perpendicular to the flow through the filter. Ageotropic hairy roots can and do grow in all directions [Wyslousil, et al., 1997]. Some roots thus, do not lie perpendicular to the flow, so the droplet capture efficiency is lower than that of a filter bed.

Another assumption that was made by Wyslouzil et al. (1997) was that a root bed will act like a dry filter bed. If the packing fraction of a filter bed is >0.04, liquid droplets will get caught in the spaces between the fibers and lead to clogging. Although the packing fraction of the root bed is almost always >0.04, the intermittent misting cycle allows this liquid hold-up to drain or be absorbed by the growing roots and clogging is avoided. Therefore, the root bed should act as though it were "dry".

The mist is in the form of an aerosol, so equations used to describe aerosol science were involved in developing the model. One equation that was used describes the capture efficiency of a single fiber (root) perpendicular to the flow of droplets. This equation is

$$\eta_C = 1 - \prod_i (1 - \eta_i) \qquad (2.4.1)$$

where η_c is the combined capture efficiency of all mechanisms involved, η_i is the efficiency for each individual mechanism, and Π indicates the product of $(1- \eta_i)$ for a range of i values. The three mechanisms considered for this model were diffusion, interception, and impaction. The overall capture efficiency of the bed is a function of the single fiber capture efficiency, and is described by

$$\eta_B = 1 - \frac{n}{n_0} = 1 - \exp\left[- \frac{4L\alpha\eta_C}{\pi D_f (1-\alpha)} \right] \qquad (2.4.2)$$

where η_B is the percent of droplets that remain in the bed; n_0 and n are the concentrations of mist droplets entering and leaving the bed, respectively; α is the fraction of the bed volume filled with roots; L is the length of the bed; and D_f is the diameter of the fiber (root) (Flagan and Seinfeld, 1988).

Because the calculated Reynolds number for the gas flow in the reactor was so low, models for creeping flow were used to describe gas flow through the bed. Also, in the study by Wyslouzil et al. (1997), the mean free path of the carrier gas was much less than the diameter of the roots. Therefore, the no-slip condition was used as a boundary condition for flow close to the root, while Kuwabara's (1959) model was used for the boundary condition for flow far from the root.

Mist droplets travel in streamlines around single roots. Sometimes, if the diameter of the droplet is large enough and the streamline is close enough to the root, the droplet will hit the root. The percentage of droplets hitting the root in this manner that are deposited on the root is the capture efficiency due to interception, η_{Int}.

Impaction, another mechanism of mist deposition, increases the overall deposition efficiency. It is a result of inertia acting on mist droplets. If droplets followed streamlines exactly, they would go around the roots, but inertia causes some of them to veer off their trajectories and continue in a straighter path. This causes more of the mist droplets to hit the roots. For the development of this model, the deposition efficiencies due to impaction and interception have been lumped together, and Crawford's (1976) method was used to solve for it. This method involves simultaneously solving the following two equations:

$$\frac{2y_1}{D_f} = \frac{1}{Ku}\left(1+\frac{2y_2}{D_f}\right)\left[2\ln\left(1+\frac{2y_2}{D_f}\right)-1+\alpha+\frac{1-\frac{\alpha}{2}}{\left(1+\frac{2y_2}{D_f}\right)^2}-\frac{\alpha}{2}\left(1+\frac{2y_2}{D_f}\right)^2\right] \qquad (2.4.3)$$

and

$$\frac{2y_1}{D_f} = \left(1+\frac{D_p}{D_f}\right)+St\sqrt{\alpha}\left[\left(\frac{1+\frac{2y_1}{D_f}}{\frac{2y_2}{D_f}}\right)\left(1+\frac{2y_2}{D_f}-\frac{2y_1}{D_f}\right)\right]\times\left[1-\exp\left(\frac{-1}{St\sqrt{\alpha}}\left(\frac{1+\frac{2y_1}{D_f}}{\frac{2y_2}{D_f}}\right)^{-1}\right)\right]-\left(1+\frac{2y_2}{D_f}-\frac{2y_1}{D_f}\right) \qquad (2.4.4)$$

where y_1 is the distance the particle's streamline is away from the imaginary line that would cut through the center of the root; y_2 is the distance between the same streamline and the root at the point when the mist droplet would cross the top of the root; D_p is the diameter of the mist droplet; Ku is the Kuwabara number, Ku = $\alpha - (¾) - (\alpha^2/4) -$

(½)ln(α); and St is the Stokes number, which is the ratio of the stopping distance of the droplet to the diameter of the root and is calculated by

$$St = \frac{D_p \rho_p C_c U_0}{18 \mu D_f} \qquad (2.4.5)$$

where ρ_p is the density of the mist droplet; μ is the viscosity of the mist droplet; U_0 is the velocity of the droplets through the root bed; and Cc is the Cunningham slip correction factor, which is calculated by

$$C_c = 1 + Kn\left[1.257 + 0.4\exp\left(\frac{-1.1}{Kn}\right)\right] \qquad (2.4.6)$$

where Kn is the Knult number.

Once equations (3) and (4) are solved, $\eta_{Imp+Int}$ can be calculated as

$$\eta_{\mathrm{Im}p+\mathrm{Im}t} = \frac{2y_1}{D_f} \qquad (2.4.7)$$

The final method by which mist droplets are deposited on roots is diffusion, the random movement of molecules. The deposition efficiency due to diffusion is described as

$$\eta_D = 3.68(2Ku)^{-1/3} Pe^{-2/3} \qquad (2.4.8)$$

where Pe is the Peclet number,

$$Pe = {U_0 D_f}/{D} \qquad (2.4.9)$$

In this equation, D is the particle diffusivity and is given by

$$D = {kTC_C}/{3\pi\mu D_P} \qquad (2.4.10)$$

where k is the Boltzmann constant and T is temperature.

When the previous equations are solved for different reactor parameters, graphs can be obtained that show how droplet efficiency will change with respect to different parameters. For example, Figure 2.4.1 shows how deposition efficiency changes with respect to packing fraction using the parameters that were specified for this project.

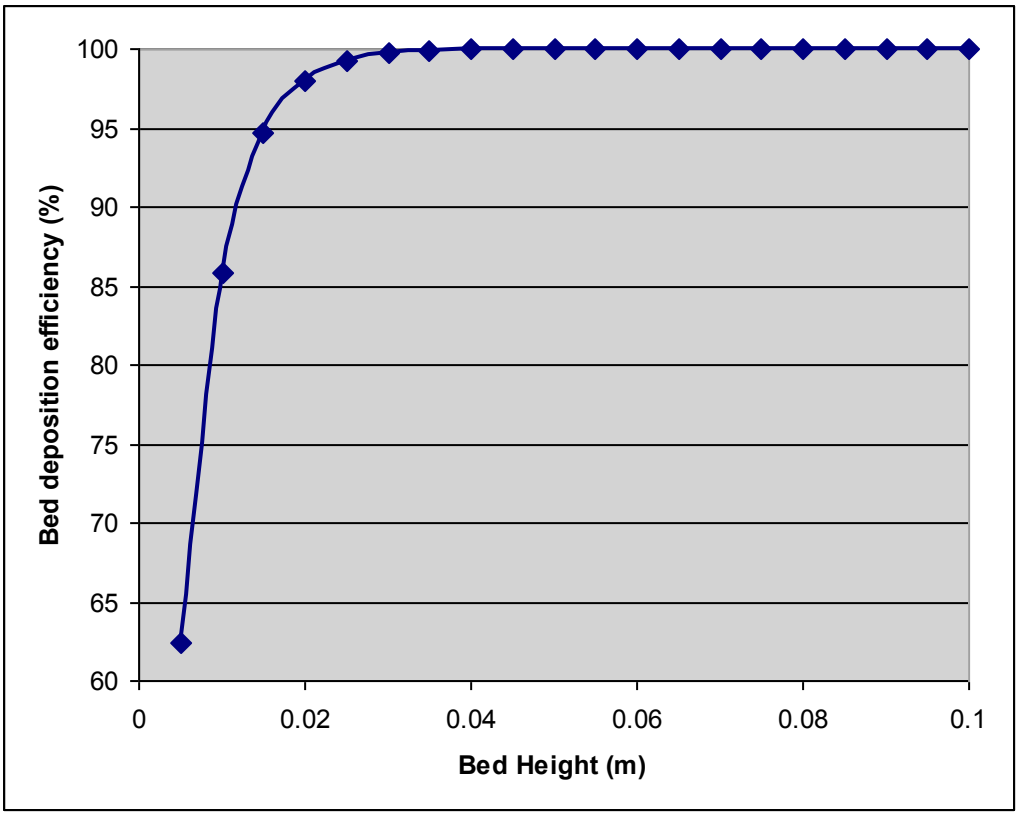

Figure 2.4.1. Effects of bed height on mist deposition at α=0.5.

Recently, Kim, et al. (2001, 2002a) did a lot of work comparing the performance of liquid- and gas-phase bioreactors, in particular bubble column and nutrient mist reactors (Figures 2.4.2a and b, respectively). Those studies showed that liquid-phase reactors produced more biomass than mist reactors, and used the mist deposition model to explain these results.

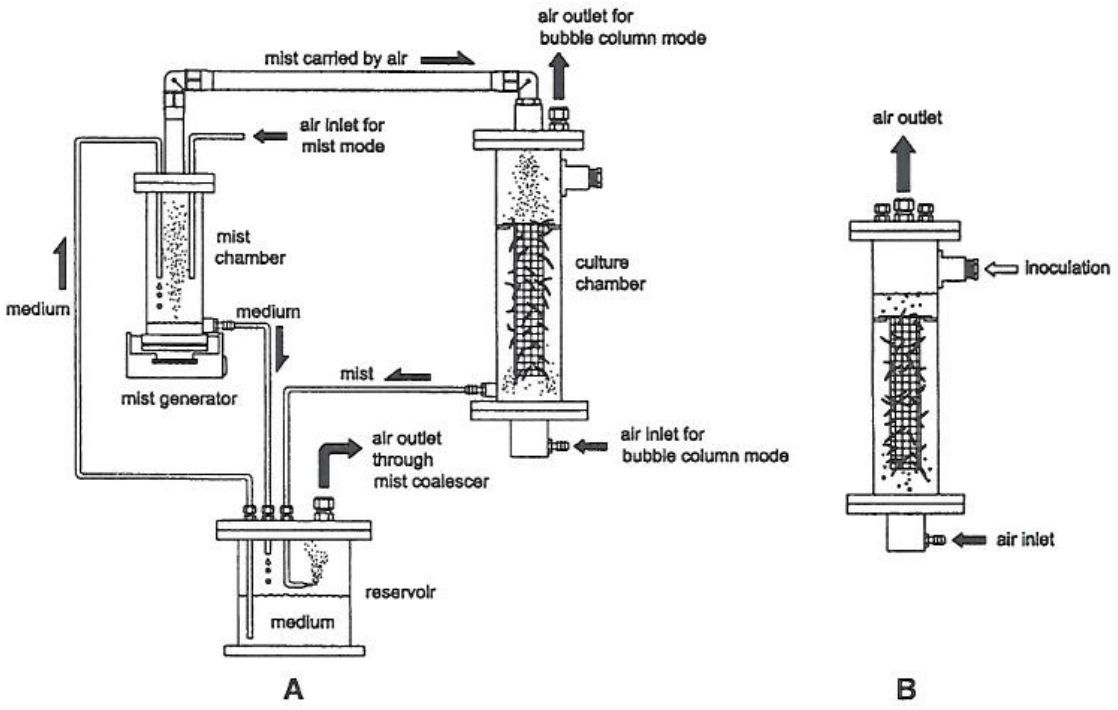

Figure 2.4.2. Mist reactor (A) and bubble column (B) used by Kim, et al. (2001)

In these experiments, more than 10 bubble column reactors and mist reactors were run concurrently, harvested, and compared for growth and secondary metabolite (artemisinin) production. Both reactors were initiated in bubble column mode to make sure the root packing density was comparable. After a designated amount of time (6-21 days) the mist reactor was drained and mist operation mode began. In both reactor types, roots were immobilized on a cylindrical stainless steel mesh, so very low initial packing densities were used. While biomass production and average specific growth rate were significantly higher in bubble-column reactors [Kim, et al., 2001, 2002a], artemisinin production was higher in nutrient mist reactors [Kim, et al., 2001]. On average, roots grown in mist reactors produced about 3 times as much artemisinin as roots grown in the bubble-columns.

To explain the low growth rates in the nutrient mist bioreactors, Kim et al. (2002a) calculated the volume of medium required by the roots to sustain growth (V_{req}), and then used the mist deposition model to calculate the volume of medium actually being deposited (V_{dep}) on the roots for several growth rates. For high growth rates such

as 0.22 day^{-1} (the average specific growth rate for roots grown in shake flasks) or 0.12 day^{-1} (the average specific growth rate for roots grown in bubble column reactors), V_{req} was greater than V_{dep} in the nutrient mist bioreactors. This shows that with Kim et al.'s (2002a) experimental setup, these growth rates cannot be achieved in mist reactors because an insufficient volume of medium is deposited on the roots, and they starve. However, if experimental parameters were altered in a way that would increase V_{dep}, higher growth rates could be possible.

They also found that the average specific growth rate was constant in nutrient mist bioreactors, but decreased with increasing packing fraction for bubble-column reactors. For all their experiments, the average specific growth rate was higher in the bubble-column than the nutrient mist bioreactor. These results were unexpected and it was assumed that roots in the mist reactor were not receiving enough liquid nutrients.

According to the mist deposition model, increasing the initial packing fraction, α, should increase the capture efficiency of the root bed, and therefore should increase the growth rate. Also, increasing the amount of sugar fed to the roots, C_S, should increase growth. To test these hypotheses, Towler et al. (2006) built a modified mist reactor that had a very small culture growth chamber. This was done to facilitate the rapid establishment of root beds of different packing densities.

Towler, et al. (2006) used a culture growth chamber with a diameter of ~30mm (Figure 2.4.3). The inoculum was 14 – 15 day old cultures of transformed (hairy) roots of *Artemesia annua*. The reactor ran on a 15 minute on/ 15 minute off cycle for up to 6 days. During the "on" cycle, 4 L min^{-1} air and 0.88 mL min^{-1} filter-sterilized Gambourg's B5 media with 3% w/v sucrose were fed to the culture growth chamber.

Figure 2.4.3. Nutrient mist bioreactor used by Towler, et al. (2006), and a harvested root mass they were able to achieve (α=0.71). Arrow indicates growth culture chamber.

In these experiments, Towler, et al. (2006) observed a growth rate of 0.12 day^{-1}, as opposed to 0.07 day^{-1} that was observed by Kim, et al. (2002a). In a separate run, Towler, et al. (2006) let the mist reactor run for 10.3 days with an initial packing density, α, of 0.39. In this experiment, the packing fraction increased to 0.71, and the average specific growth rate was 0.11 $days^{-1}$. When *Cs* was increased from 3% to 5% sucrose, the average specific growth rate further increased to 0.20. Taken together these data showed that higher average specific growth rates and high final biomass densities can be achieved in nutrient mist bioreactors if higher initial α, and *Cs* are used.

The object of this project was to model the mist deposition and make predictions of growth rates in an altered, scaled-up version of Towler, et al.'s (2006) nutrient mist bioreactor where the mist deposition is no longer slaved to the input air flow rate.

2.5 Calculations can be made to develop an effective mist reactor based on the mist-deposition model.

Towler et al. (2006) demonstrated that high growth rates and biomass densities could be achieved in the nutrient mist bioreactor. The reactor developed for this project is to be a larger version of the one used by Towler, et al. (2006), to examine scale-up

possibilities. There are several important changes to the design, the most important of which are the use of a new misting system and larger growth chamber.

In the old system, there were three major components: a culture medium reservoir, a mist generator chamber, and a growth chamber (Figure 2.4.3). That version used a mist generator that used ultrasonic energy to generate mist droplets with an average diameter of ~7-10μm (Weathers, et al., 1999). Air was piped into the mist generator chamber in order to transport the droplets into the culture growth chamber. The new system uses a spray nozzle to generate mist droplets that average ~20μm in diameter with an exit velocity of 110 m s^{-1} [Plant Fog, 2006] with delivery directly into the culture chamber. Therefore, there is now a separation of air and droplet streams because the new mist reactor does not need an air stream to transport droplets from the mist generator chamber to the growth chamber (Figure 2.5.1). The new system contains 1 growth chamber and two culture medium reservoirs. One medium reservoir sits below the rest of the reactor, and allows media to flow down into it from the growth culture chamber. Media is then pumped to the second reservoir, which sits at the same level as the culture growth chamber. Media is gravity fed from the second reservoir through a pump and into the chamber. Air must be supplied to the reactor separately, so a second inlet was drilled into the top of the culture growth chamber. Considering that Williams and Doran (2004) showed that there was improved fluid motion in root beds with co-current flow of liquid and air, air in the newly designed mist reactor should enter through the top of the chamber adjacent to the inlet port for the mist droplets (Figure 2.5.1).

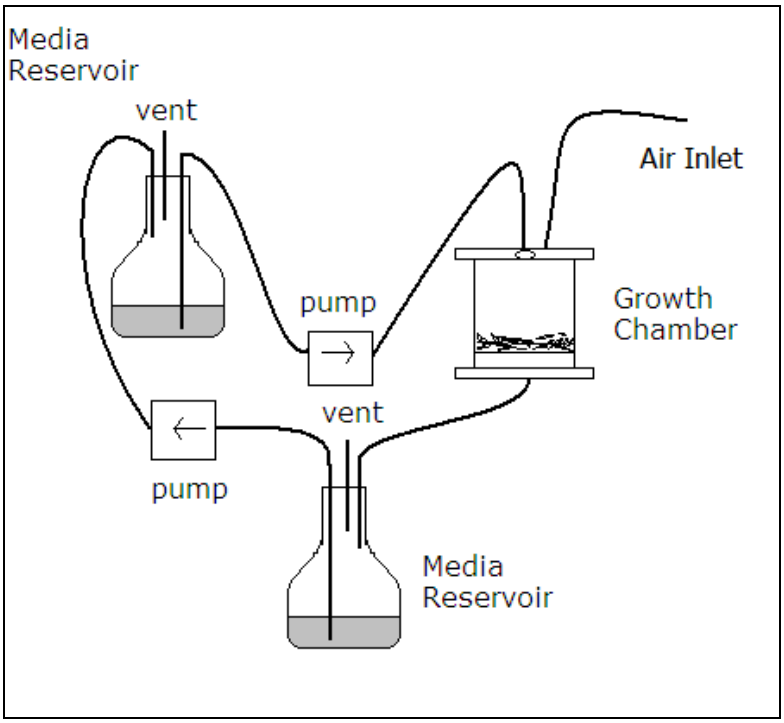

Figure 2.5.1. Schematic of my reactor.

In the previous mist reactor used by Towler, et al. (2006), the mist was deposited into the root bed by a gas flow that carried the mist droplets from the generating chamber to the culture growth chamber (Figure 2.4.1). Because mist delivery was slaved to gas delivery in earlier versions of the mist reactor, the purpose of this project was to study the effects of decoupling the air from the mist delivery and also the effects of varying the air flow rate.

Table 2.5.1. Parameters used for experimental settings.

Parameter	Value	Units
Density of gas	1.225	kg m^{-3}
Viscosity of gas	1.72e-05	kg m^{-1} s^{-1}
Temperature	293.15	K
Pressure	1	atm
Gas flow rate	4	L min^{-1}
Packing fraction	0.19	
Root diameter	0.0005	m
Media flow rate	0.000035	m^3 min^{-1}
Mist drop diameter	0.00002	m
Mist drop velocity	110	m s^{-1}
Media cone angle	80	Degrees

In order to calculate the dimensions of the culture growth chamber and the mist deposition efficiencies, certain parameters had to be specified. These parameters are shown in Table 2.5.1. The density and viscosity of the gas are general properties of room air. All experiments were conducted at standard temperature and pressure. The gas flow rate and the initial packing fraction were taken from the experiments of Towler, et al. (2006). The root diameter is the average root diameter for *Artemisia annua* roots. The media flow rate, mist droplet diameter, mist droplet velocity, and media cone angle are all properties of the misting system. MATLab was used to calculate the dimensions of the reactor growth chamber, and the .m file is attached as an Appendix.

Figure 6 shows the spray cone of mist particles formed by the spray nozzle. The mist particles have an initial velocity of 110 m s^{-1}[Plant Fog, 2006]. The radius of the reactor was calculated using the particles on the outside of the cone. If the reactor radius is too large, the roots on the outside of the bed will starve because the nutrients will not reach them. If the radius is too small, mist will impact the wall of the culture growth chamber, form large rivulets, and slide down it. This could lead to flooding near the walls, and hence, a liquid-based reactor. The reactor radius was calculated by calculating the stopping distance, the distance the mist particles will travel in the r-direction before they stop and drop vertically in the z-direction, for the particles on the outside of the cone. First, the stopping distance in the r-direction was calculated using the equation

$$SD_r = T_{char} * (v_r - v_g) \qquad (2.5.1)$$

where SD_r is the stopping distance in the r-direction, T_{char} is the characteristic time in seconds, v_r is the velocity of the mist particles in the r-direction, and v_g is the velocity of the gas. T_{char} was calculated by

$$T_{char} = \frac{m_p}{3\pi\mu D_p} \qquad (2.5.2)$$

where m_p is the mass of a mist particle, and μ is the viscosity of the air. v_r was calculated by

$$v_r = v_p \sin(\frac{\theta}{2}) \qquad (2.5.3)$$

where v_p is the velocity of the particle, and θ is the angle of the spray cone. The diameter of the culture growth chamber is 2 times the stopping distance in the r-direction, which was found to be 16cm. A 16cm-diameter chamber was not available, so a 14cm chamber was used instead and the mist nozzle was placed above the root bed accordingly (Figure 2.5.2).

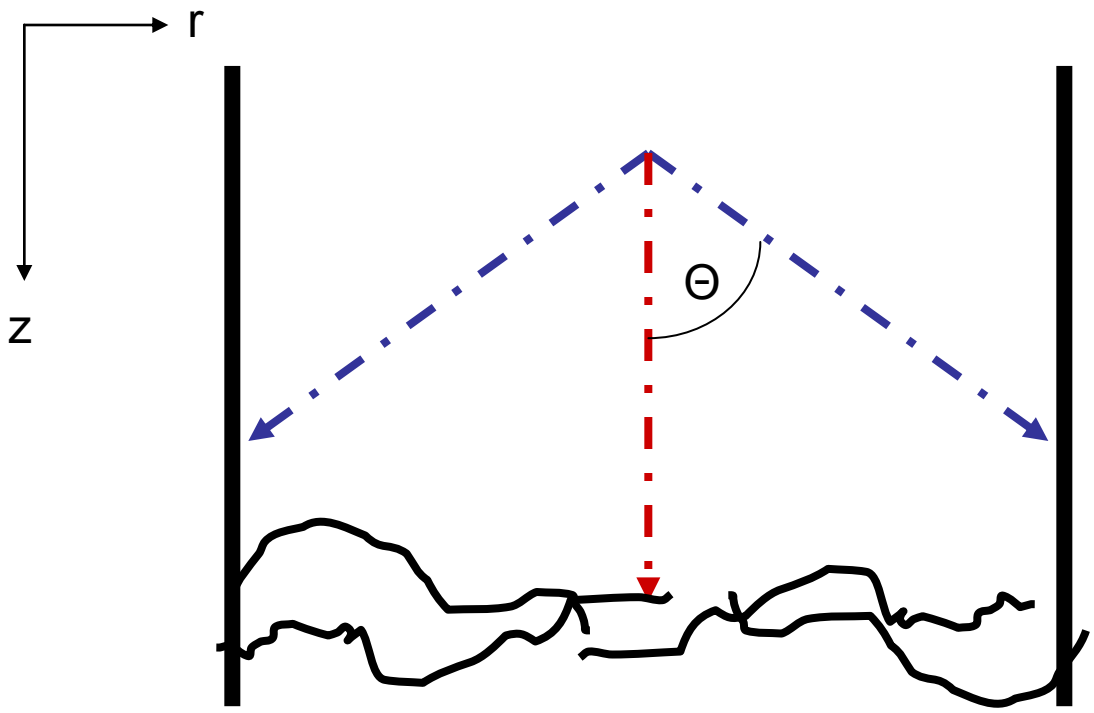

Figure 2.5.2. Mist spray patterns (Wyslouzil, 2005)

In order to determine the height the nozzle should be above the root bed, the velocity of the particles traveling in the z-direction was considered (Figure 2.5.2). The mist particles should be carried into the root bed by the air. The stopping distance, the distance the mist particles travel downward before they slow down and travel at the same velocity as the air is the distance the spray nozzle should be above the root bed.

$$SD_z = T_{char} * \left(v_p - v_g\right) \qquad (2.5.4)$$

where v_p is the velocity of the mist droplets. This distance was calculated to be 14cm.

To determine the depth of the test bed of roots, the mist deposition model was used. Figure 2 shows the mist deposition model plotted as a function of bed depth for the system parameters chosen. A depth of 4cm was used for these experiments. Theoretically 100 percent of the mist particles should be deposited on the roots. If a

larger bed depth were chosen, 100 percent of the mist particles would be deposited, but there may not be enough nutrients to penetrate into the entire bed to feed the bottom roots. Therefore, we also calculated the volume of media deposited on the roots, V_{dep}, and the volume of media required by the roots to grow, V_{req} (Kim, et al., 2002a). Both volumes are in mL day^{-1}.

The equation for V_{dep} is

$$V_{dep} = 24\omega Q_L \eta_B \qquad (2.5.5)$$

where 24 is the conversion from hours to days, ω is the duty cycle (15 min hr^{-1} for a 5 min on/ 15 min off), Q_L is the medium flow during the on cycle (mL min^{-1}), and η_B is the deposition efficiency of the root bed. V_{req} is calculated by

$$V_{req} = 10^6 \rho_{FW} \cdot \frac{DW}{FW} \cdot \frac{\mu}{C_S} \cdot \frac{1}{Y_{X/S}} \cdot V \cdot \alpha \qquad (2.5.6)$$

where ρ_{FW} is the density of fresh roots (g FW ml^{-1}), DW/FW is the ratio of dry weight to fresh weight, μ is the specific growth rate (day^{-1}), C_S is the sugar concentration in the medium (g L^{-1}), $Y_{X/S}$ is the apparent biomass yield of the limiting nutrient (sugar) (g DW biomass / g nutrient), V is the working volume of the reactor (L), and α is the packing fraction.

The value for $Y_{X/S}$ was taken to be 0.35, which was determined in shake flasks (Kim, 2001). The DW/FW ratio was assumed to be 0.055, which was the lowest value obtained by Kim, et al. (2002a). C_S for our studies is 30 g L^{-1} and μ was assumed to be 0.12 day^{-1}, which was the growth rate observed by Towler, et al. (2006).

Figures 2.5.3a-d show V_{dep} and V_{req} as functions of the bed height for α = 0.19, and α = 0.71. These are the minimum and maximum packing densities either used or achieved by Towler, et al. (2006). These graphs show that even at high packing densities, the volume of media deposited in the root bed is much greater than the volume of media required. Therefore, roots should grow well.

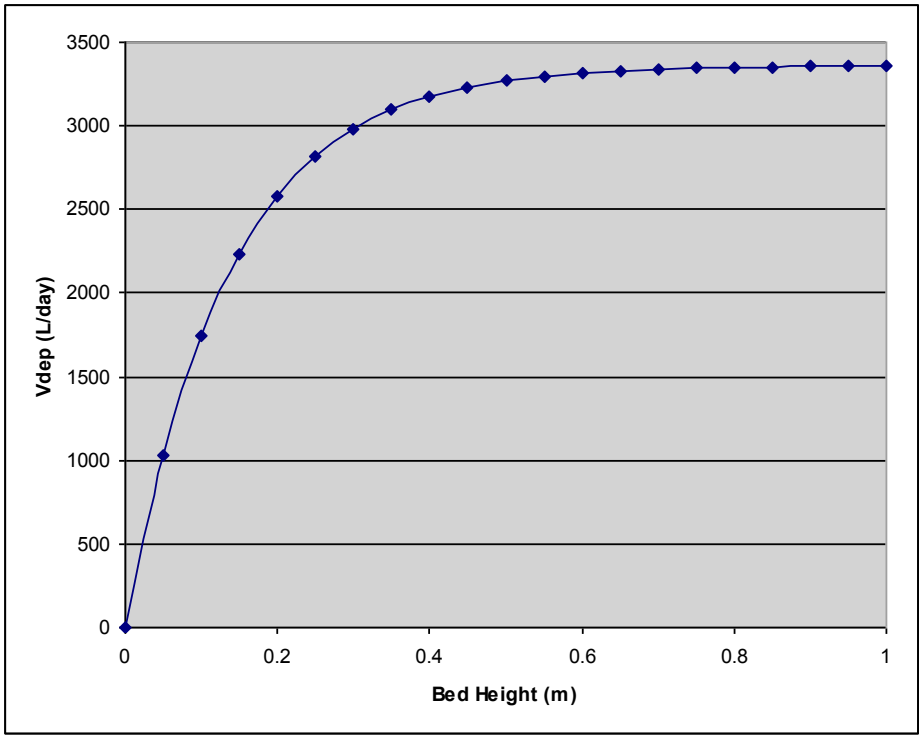

Figure 2.5.3a. V_{dep} as a function of bed height for α=0.19.

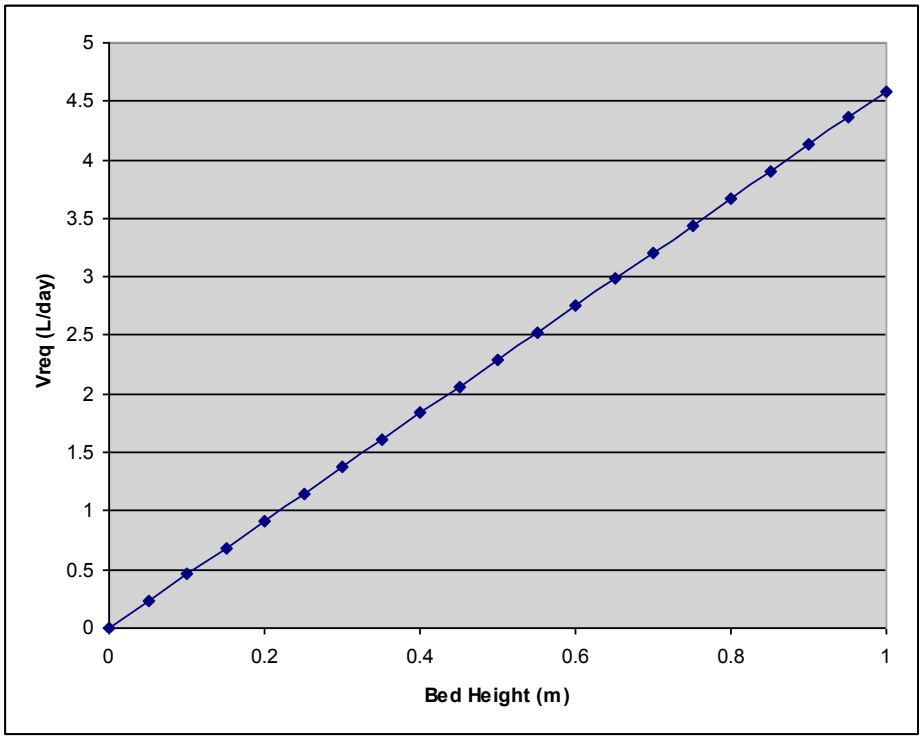

Figure 2.5.3b. V_{req} as a function of bed height for α=0.19.

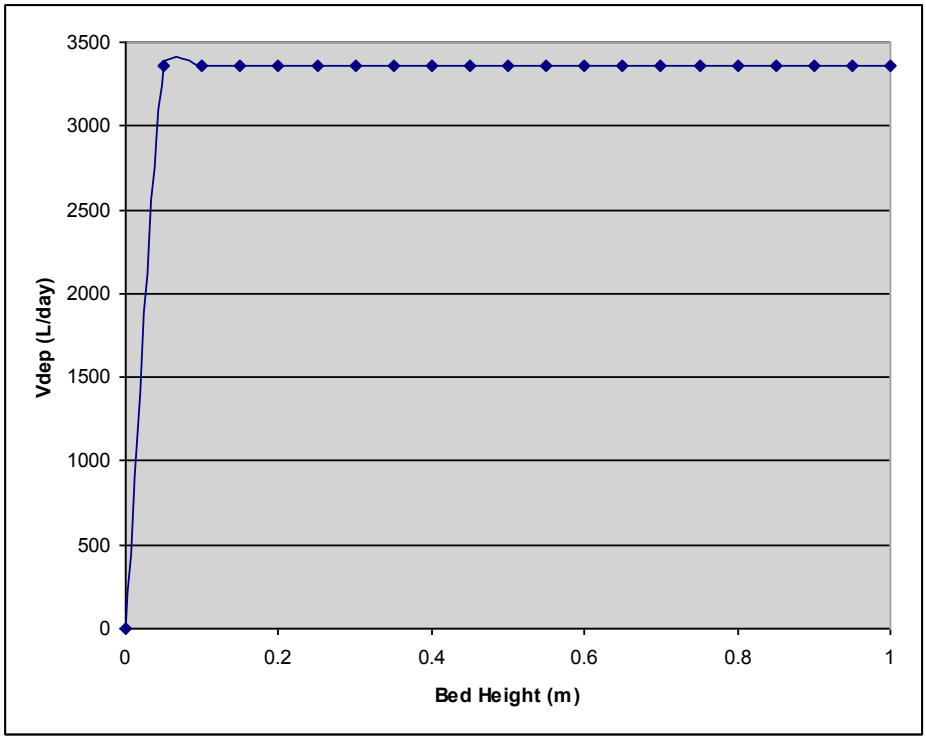

Figure 2.5.3c. V_{dep} as a function of bed height for α=0.71.

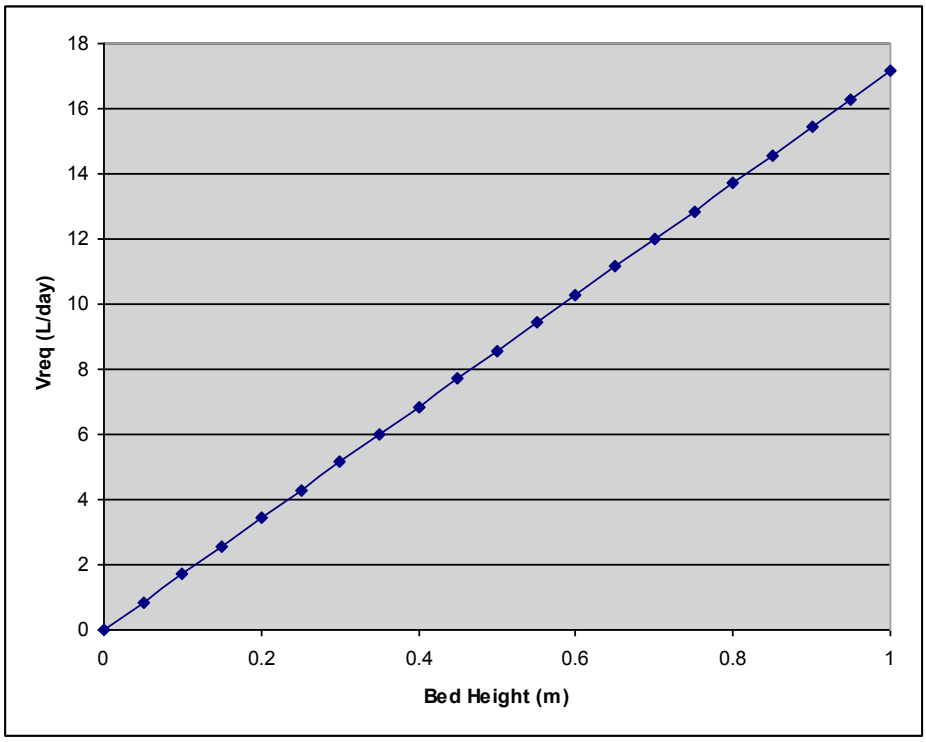

Figure 2.5.3d. V_{req} as a function of bed height for α=0.71.

The misting system used in this project (Plant Fog "Tropic-IP65") is very different from the misting system used by Towler et al. (2006). In the old system,

ultrasonic energy is used to generate mist droplets, and an air stream carries the mist droplets from the mist generation chamber to the culture growth chamber. In the new system, media is fed through a microfilter (Figure 2.5.4), then is pumped using a high pressure pump (Plant Fog "tropic" pump) (Figure 2.5.5) to the nozzle (Figure 2.5.6). No air flow is used to promulgate the droplets in this misting system.

Figure 2.5.4. Misting system microfilter (Plant Fog, 2006).

Figure 2.5.5. Misting system pump (Plant Fog, 2006).

a.

b.

Figure 2.5.6. Misting system nozzle (a) and spray cone (b) (Plant Fog, 2006).

Other than the larger reactor diameter, different misting system, and different bed height, the experimental parameters were the same as those used by Towler, et al. (2006), and are shown in Table 2.5.1. The parameter that was to be studied was gas flow rate, and the effect of being decoupled from the air. Figures 2.5.7 and 2.5.8 show the effect of gas flow rate on mist deposition efficiency when the gas is coupled with the mist delivery, according to the mist deposition model. Figure 11 shows that for gas flow rates less than 2 L min^{-1} and $\alpha = 0.19$, mist deposition should decrease with an increase in gas flow rate. For flow rates greater than 2 L min^{-1}, the mist deposition efficiency increases with an increase in gas flow rate. Figure 12 shows that with $\alpha = 0.71$, there is 100 % mist deposition, regardless of the gas flow rate.

For our reactor setup, the mist flow was decoupled from the gas flow. For zero gas flow rate, the mist particles will travel at their own velocity, 110 m s^{-1}. However, once the gas flow is added, the mist particles should travel at the velocity of the gas, and therefore should follow the mist deposition model.

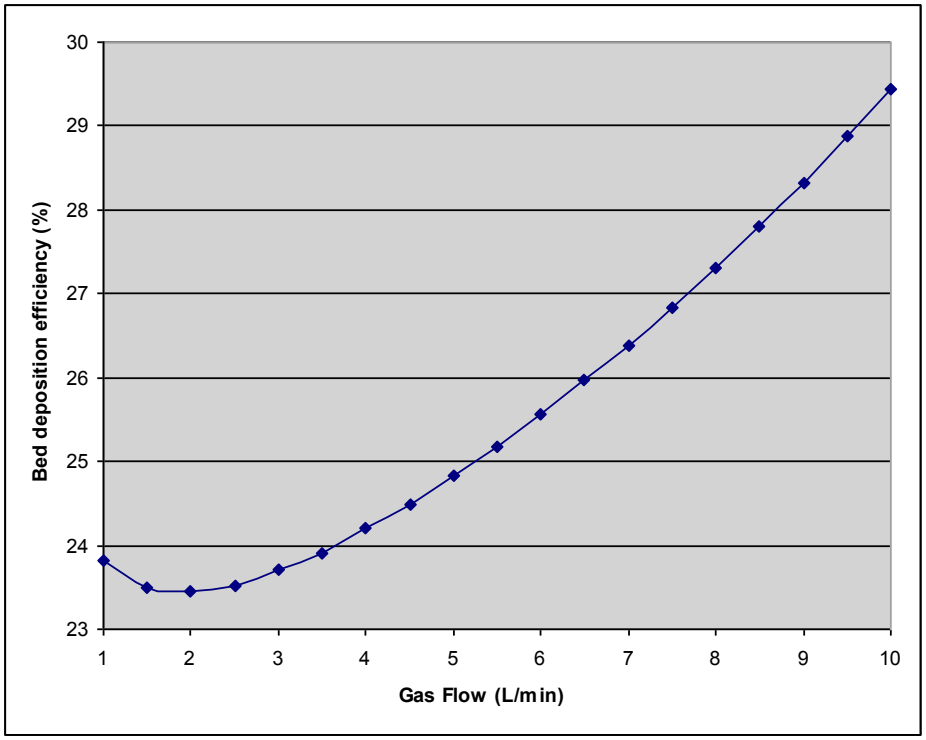

Figure 2.5.7. Effect of gas flow rate on bed deposition efficiency for α =0.19.

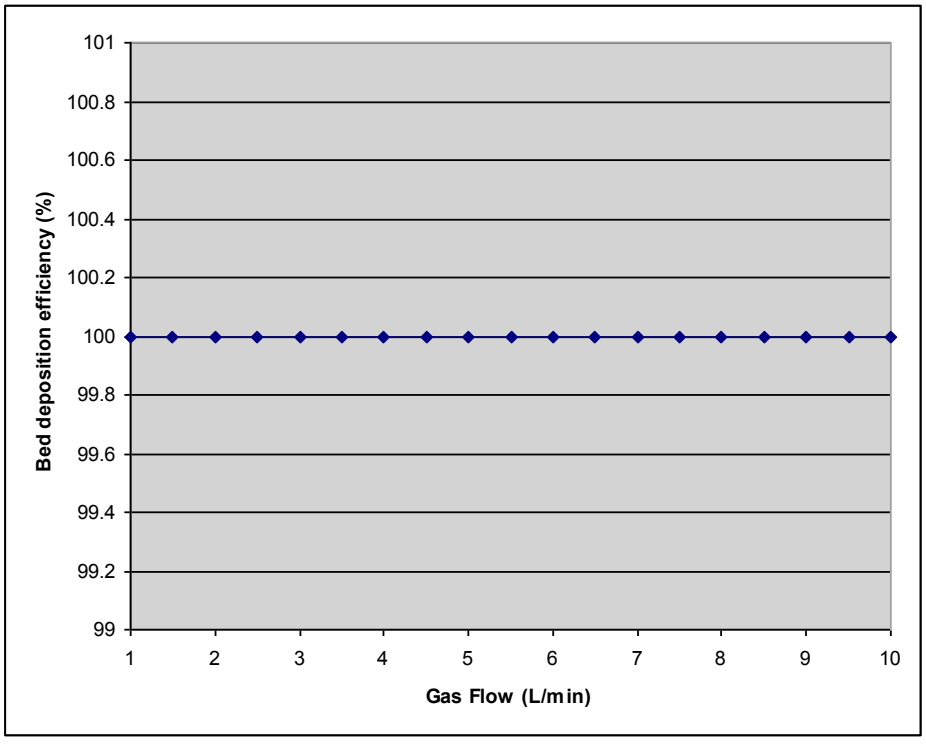

Figure 2.5.8. Effect of gas flow rate on bed deposition efficiency for α =0.71.

3. HYPOTHESES

Prior research conducted by Towler (2005) and calculations made using the mist deposition model [Wyslouzil, et al., 1997] have led to the following hypotheses:

1. If the gas flow rate is increased in a scaled-up mist reactor having a mist flow now separated from the gas flow, the deposition efficiency in the root bed will also increase, until it reaches 100%.
2. If the deposition efficiency increases, the average growth rate in this scaled-up reactor will also increase.

4. OBJECTIVES

There are two main objectives for growing roots in this larger version of the nutrient mist bioreactor:

1. To successfully grow hairy roots of *Artemisia annua* in this larger scale nutrient mist bioreactor without contamination.
2. To calculate the growth rate at several gas flow rates, and thus determine the relationship between growth rate and gas flow rate, thereby testing the above hypotheses.

5. MATERIALS AND METHODS

5.1 Cultures and their maintenance

This project used transformed roots of *Artemisia annua* (clone YUT16) [Weathers, et al., 1994]. Roots were first grown on plates containing semi-solid B5 medium [Gamborg, et al., 1968] with 3% w/v sucrose and 0.23% w/v Phytagel. The pH of the media was adjusted to 5.7 before autoclaving. The plates were incubated in the dark at a temperature of 23±2ºC. After growing on the plates for one month, the roots were transferred to 125mL shake flasks with 50mL of liquid B5 medium and 3% (w/v) sucrose. The flasks were kept on a shaker at 100rpm, at 23±2ºC, with cool white fluorescent light for 14 days before being subcultured into fresh B5 medium in shake flasks. Roots were grown for another 14 days before inoculation.

5.2 Reactor and concurrent shake flask culture

The nutrient mist bioreactor that was used for this project is a modified version of the reactor used by Towler (2005) (Figure 4). A chamber with a 14cm diameter was used as opposed to the 27mm-diameter chamber used previously. The chamber was constructed of clear polycarbonate. Also, a new misting system was used in this reactor. This new system used a high-pressure fogging (Plant Fog model K-100) nozzle to supply only media (no air), whereas the old system delivered the media as droplets being carried by air to the reactor. Although the air was supplied separately, it was on the same duty cycle as the mist. The new nozzle produced droplets with a reported (by Plant Fog) average diameter of 20µm (instead of the 7-10 µm particles that were produced using the old system). A Grelab 451 220V timer was used to regulate the misting cycle of 2 min on / 1 min off (instead of 15min on / 15 min off). The air was humidified and sterilized by being passed through a 0.2 micron sterile filter before entering the reactor. The air was also on a Grelab 451 timer and cycled with the media. All media used for these experiments was filter sterilized to eliminate the degradation of sucrose that occurs during autoclaving and minimize clogging of the misting nozzle [Weathers, et al., 2004].

5.3 Root Culture

Roots were harvested from 14 day shake flask cultures. In a sterile transfer hood, 116g FW of roots were blotted and weighed into four 250mL beakers, and 45mL of B5 media was added to keep the roots alive. Then 0.5g FW of roots were weighed into each of 4 100mL beakers and 5mL of media was added. The eight beakers were kept on a shaker while the reactor was sterilized.

5.4 Sterilizing the reactor system

The reactor chamber and both media reservoirs were autoclaved as three separate pieces at 121°C for 40 minutes. The misting system cannot be autoclaved, so it was chemically sterilized. In a sterile transfer hood, 500mL sterile 70% ethanol was pumped through the misting system. The misting cycle was 2 minutes on, 1 minute off. During several "off" periods, the misting head was soaked in sterile 70% ethanol to sterilize the surface. This was followed by pumping about 300mL sterile water through the system to rinse the ethanol out. Once the mister was sterilized, the system was assembled in the sterile transfer hood.

5.5 Putting the system together

In a sterile transfer hood, the two media reservoirs and reactor chamber were connected to each other. One liter of sterile B5 medium with 3 % w/v sucrose was added to the second reservoir and 1mL of Plant Preservation mixture (PPM) was added to the medium to keep it from getting contaminated. Using large forceps sterilized with 70% ethanol, roots were then manually packed into the chamber at a packing density, α, of 0.19, previously determined by Towler (2005) to be the minimum α at which roots no longer compacted., The roots were evenly distributed upon the wire mesh inside the chamber to a depth of 4cm. The entire reactor system was then moved to a room kept at 25^{o}C in constant light for the 6-day experiment. A set of shake flasks were grown at the same temperature and light conditions for comparison, and were inoculated with 0.5g FW roots in each of 4, 125mL flasks with 50mL B5 media.

6. RESULTS AND DISCUSSION

Before roots could be cultured in this reactor, the system had to be evaluated for leaks and then run with sugar-containing culture medium to see if the chemical sterilization procedure was adequate. The first part of the reactor testing was a "dry run". Here, the reactor was set up and run with no inoculum, but with filtered water in the place of medium. This run exposed a leak in the connection between the bottom of the culture growth chamber and the tubing that led to the media reservoir. The nozzle worked as expected and produced a cone of predicted dimensions (Figure 2.5.2) and fine mist particles that covered the walls of the culture growth chamber.

The success of this run was an important first step and led to the second test run, which was identical to the first only instead filtered B5 medium with 3% sucrose was used. The importance of this run was to test our sterility techniques before inoculating the culture growth chamber with roots. The reactor ran for 6 days. At the end of the run, a sample from the media reservoir was streaked onto a plate of semi-solid B5 medium and incubated at 23±2^{o}C. No microbial growth was observed on the plate after 30 days of incubation. This run did not get contaminated, and thus demonstrated that the sterilization techniques were successful.

After the first two runs were successfully completed, the first run with inoculum was initiated. The reactor was sterilized and inoculated with roots, and ran for 10h. At this point, it was observed that the pump had cavitated resulting in its permanent failure; no more experiments could be run. The reactor was left up for several days without contamination. These results further strengthened our argument that the sterilization techniques worked.

7. CONCLUSIONS

A very important conclusion can be drawn from the modeling analysis above. If the experiments had been completed, the volume of media deposited in the root bed would always be greater than the volume of media required by the roots to survive. This prediction is important because it suggests that root growth should not be limited by a lack of liquid-phase nutrients. Due to the fact that the root bed will be in a gas-phase reactor, the roots will also have an ample supply of gas-phase nutrients. This situation should be conducive to root growth, and therefore, the bioreactor set-up should be an effective way to grow hairy roots.

Another important conclusion that was drawn from this project is that the sterilization techniques developed for this reactor and used in the first three runs of this project are successful. It is possible to keep the reactor void of microbes that will interfere with root growth and secondary metabolite production.

When these studies are eventually conducted, and the same reactor set-up and sterilization techniques are used, the reactor should successfully grow roots of *Artemesia annua*. Then the effects of separating the gas flow from mist delivery could definitely be analyzed, and the model described in this report empirically confirmed.

APPENDIX A1: MATLab file for culture growth chamber dimension calculations.

```
clear all;

%Basic parameters

rho=1.225; %density of carrier gas (kg/m^3)
mu=1.72e-05; %air viscosity in kg/(m s)
Df=0.0005; %diameter of the root (m)
Qm=0.000035; %flow of media (m^3/min)
T=293.15; %temperature
Dp=0.00002; % diameter of particle (m)
rhop=1000; %density of particle (kg/m^3)
k=1.3806065e-23; %Boltzmann constant (m^2*kg/s^2*K)
y=6.51e-8; %mean free path of gas (m)
QgENGLISH=.1:.1:4; %gas flow (L/min)
alpha=0.19; %packing density
L=0.05; %height of bed

% Convert gas flow to metric

Qg=QgENGLISH.*.001/60 %gas flow (m^3/s)

% Stopping distance parameters

velP = 110; %particle velocity (m/s)
Dt = 0.004318; %diameter of gas tube (m)
volP = 4/3*pi*(Dp/2)^3; %particle volume (m^3)
massP = volP*rhop; %mass of particle (kg)

% Calculate gas velocity

ATube = pi*(Dt/2)^2; %cross-sectional area of gas tube (m^2)
velG = Qg./ATube; % gas velocity in the supply tube(m/s)
charT = massP/(3*pi*mu*Dp); %characteristic time (s)
stopD = charT.*(velP-velG) % height of nozzle above bed (m)
angle = 80; %angle of cone (%)

% Calculate velocity in r and z directon, stopping distance, and optimum
% bed diameter

velR = velP*sin((90-angle/2)*pi/180); %velocity in r-dir (m/s)
velZ = velP*cos((90-angle/2)*pi/180); %velocity in z-dir (m/s)
stopDR = charT.*(velR-velG); %stopping distance for the particles r-dir (m)
d = 2.*stopDR %diameter of bed (m)
```

```
% Calculations for the mist deposition model.

A=pi.*d.^2./4; %cross-sectional area of the bed (m^2)
Vo=Qg./A; %Gas velocity through bed (m/s)
Re=rho.*Vo.*Df./mu; %Reynold's number
Ku=alpha-(3./4)-((alpha.^2)./4)-.5*log(alpha);
Kn=2.*y./Df;
Cc=1+Kn.*(1.257+.4.*exp(-1.1./Kn));
D=k.*T.*Cc./(3.*pi.*mu.*Dp);
Pe=Vo.*Df./D;
St=Dp.^2.*rhop.*Cc.*Vo./(18.*mu.*Df);

% Solve the two equations for y1 and y2.

y2=ones(1,length(Qg)).*1e-5; % initial guess for y2
answer=ones(1,length(Qg)).*3; %initial value for "answer"
y1=ones(1,length(Qg)); % initial guess for y1
x=1; % Counter

while x<length(Qg)+1

   while answer(x)>2
      y2(x)=y2(x)+1e-8;
      y1(x)=((1./Ku(x)).*(1+2.*y2(x)./Df).*(2.*log(1+2.*y2(x)./Df)-1+alpha(x)+(1-
alpha(x)./2)./((1+2.*y2(x)./Df).^2)-(alpha(x)./2).*((1+2.*y2(x)./Df).^2))).*(Df./2);

answer(x)=((1+Dp./Df)+St.*alpha(x).^.5.*((1+(2.*y1(x)./Df)./(2.*y2(x)./Df)).*(1+2.*y2(
x)./Df-2.*y1(x)./Df)).*(1-exp(-
1./(St.*alpha(x).^.5).*(1+(2.*y1(x)./Df)./(2.*y2(x)./Df)).^(-1)))-(1+2.*y2(x)./Df-
2.*y1(x)./Df)).*(Df./y1(x));
   end

   x=x+1;
end

% Solve for deposition efficiencies.

etaI=2.*y1./Df; % Capture efficiency due to Impaction and Interception
etaD=3.86.*(2.*Ku).^(-1./3).*Pe.^(-2./3); % Capture efficiency due to Diffusion
etaC=1-(1-etaI).*(1-etaD); % Capture efficiency of a single fiber (root)
etaB=(1-exp(-(4.*L.*alpha.*etaC)./(pi.*Df.*(1-alpha)))).*100; % Overall capture
efficiency of the bed

% Solve for volume of media required and volume of media deposited.

Yxs = 0.35; % g DW/ g glucose equivalent from Kim et al.
```

```
DWFW = 0.055; % DW/FW from Kim et al.
mu2 = 0.22; % growth rate (day^-1)
Cs = 30; % g/l sugar
V =  pi.*d.^2./4.*L*1000; % reactor volume (L)
Vreq = 10.^6.*rhop.*.001.*DWFW.*mu2./Cs.*1./Yxs.*V.*alpha; % Volume of media
required by roots

omega = 40; % min/hr
etaOM = etaB; % overall mass deposition efficiency
Vdep = 24.*omega.*Qm.*10.^6.*etaB; % Volume of media deposited (I think this value
ends up way too large.)

% Plot bed deposition efficiency as a function of packing density.

plot(alpha,etaB,'bo-')
title('Effect of packing density on bed deposition efficiency')
xlabel('Alpha')
ylabel('Bed deposition efficiency %')
```

REFERENCES

Carvalho EB, Curtis WR. 1998. Characterization of fluid-flow resistance in root cultures with a convective flow tubular bioreactor. Biotechnology and Bioengineering 60:375-384.

Crawford M. *Air Pollution Control Theory*; McGraw-Hill: New York, 1976; p 424 – 433.

Gamborg OL, Miller RA, Ojima K. 1968. Nutrient requirements of suspension cultures of soybean root cells. Experimental Cell Research 50:148-151.

Ferreira JFS, Laughlin JC, Delabays N, de Magalhaes PM. Cultivation and genetics of *Artemisia annua* L. for increased production of the antimalarial drug artemisinin. 2005. Plant Genetic Resources: characterization and utilization 3.2:206-224.

Flagan RC, Seinfeld JH. *Fundamentals of air pollution engineering*; Prentice Hall: New Jersey, 1988; p 433-435.

Flores HE, Curtis WR. 1992. Approaches to understanding and manipulating the biosynthetic potential of plant roots. Annals of the New York Academy of Sciences 665:188-209.

Kim Y. 2001. Assessment of bioreactors for transformed root cultures. PhD thesis, Worcester Polytechnic Institute, Worcester, MA.

Kim Y, Wyslouzil BE, Weathers PJ. 2001. A comparative study of mist and bubble column reactors in the in vitro production of artemisinin. Plant Cell Reports 20:451-455.

Kim Y, Weathers PJ, Wyslouzil BE. 2002a. Growth of *Artemisia annua* hairy roots in liquid- and gas-phase reactors. Biotechnology and Bioengineering 80:451-464.

Kim Y, Wyslouzil BE, Weathers PJ. 2002b. Secondary metabolism of hairy root cultures in bioreactors. In Vitro Cellular and Development Biology - Plant 38:1-10.

Kuwabara S. 1959. The forces experienced by randomly distributed parallel circular cylinders or spheres in a viscous flow at small Reynold's numbers. Journal of the Physical Society of Japan 14:527-532.

McKelvey SA, Gehrig JA, Hollar KA, Curtis WR. 1993. Growth of plant root cultures in liquid- and gas-dispersed reactor environments. Biotechnology Progress 9:317-322.

Perry, R.H., Green, D.W. 1997. Perry's Chemical Engineers' Handbook (7th Edition). McGraw-Hill, New York. (pp. 14-81-14-82).

Plant Fog. Updated on 30 Jan. 2006. Referenced on 02 Feb 2006. <http://www.plantfog.at/English/framesetE.html>

Ramakrishnan D, Curtis WR. 2004. Trickle-bed root culture bioreactor design and scale-up: growth, fluid-dynamics, and oxygen mass transfer. Biotechnology and Bioengineering 88:2:248-260.

Singh G, Curtis WR. Reactor design for plant root culture. In: Shargool, P.D., Ngo, T.T., eds. Biotechnological applications plant cultures. CRC series of current topics in plant molecular biology. Boca Raton, FL: CRC Press; 1994:185-206.

Towler MJ. 2005. Effects of inoculum density, carbon concentration, and feeding scheme on the growth of transformed roots of *Artemisia annua* in a modified nutrient mist bioreactor. PhD thesis, Worcester Polytechnic Institute, Worcester, MA.

Towler MJ, Wyslouzil BE, Weathers PJ. 2006. Using an aerosol deposition model to improve hairy root growth in a mist reactor. Biotechnology and Bioengineering, submitted for publication.

Weathers PJ, Cheetham RD, Follansbee E, Teoh K. 1994. Artemisinin production by transformed roots of *Artemisia annua*. Biotechnology Letters 16:1281-1286.

Weathers PJ, Wyslouzil BE. (2000). Bioreactors, mist. In *Encyclopedia of Cell Technology.* John Wiley & Sons. NY, NY (pp. 224-230).

Weathers PJ, Wyslouzil BE, Wobbe KK, Kim YJ, Yigit E. 1999. The biological response of hairy roots to O_2 levels in bioreactors. In Vitro Cellular and Development Biology - Plant 35:286-289.

Weathers PJ, DeJesus-Gonzalez L, Kim YJ, Souret FF, Towler MJ. 2004. Alteration of biomass and artemisinin production in *A. annua* hairy roots by media sterilization method and sugars. Plant Cell Reports 23:414-418.

Williams, GRC, Doran, PM. 2000. Hairy root culture in a liquid-dispersed bioreactor: Characterization of spatial heterogeneity. Biotechnology Progress 16:391-401.

Wyslouzil BE. Personal Communication. Nov 9, 2005.

Wyslouzil BE, Whipple M, Chatterjee C, Walcerz DB, Weathers PJ, Hart DP. 1997. Mist deposition onto hairy root cultures: aerosol modeling and experiments. Biotechnology Progress 13:185-194.